ChemPubSoc Europe

DOI: 10.1002/cmdc.201900226

CHEMMEDCHEM Full Papers

# $Cu^{II}$ and $Au^{III}$ Complexes with Glycoconjugated Dithiocarbamato Ligands for Potential Applications in Targeted Chemotherapy

Nicolò Pettenuzzo,[a, b] Leonardo Brustolin,[a, b] Elisa Coltri,[a] Alberto Gambalunga,[c] Federica Chiara,[c] Andrea Trevisan,[c] Barbara Biondi,[d] Chiara Nardon,[a] and Dolores Fregona*[a]

This work is focused on the synthesis, characterization, and preliminary biological evaluation of bio-conjugated $Au^{III}$ and $Cu^{II}$ complexes with the aim of overcoming the well-known side effects of chemotherapy by improving the selective accumulation of an anticancer metal payload in malignant cells. For this purpose, carbohydrates were chosen as targeting agents, exploiting the Warburg effect that accounts for the overexpression of glucose-transporter proteins (in particular GLUTs) in the phospholipid bilayer of most neoplastic cells. We linked the dithiocarbamato moiety to the C1 position of three different monosaccharides: D-glucose, D-galactose, and D-mannose. Altogether, six complexes with a 1:2 metal-to-ligand stoichiometry were synthesized and in vitro tested as anticancer agents. One of them showed high cytotoxic activity toward the HCT116 colorectal human carcinoma cell line, paving the way to future in vivo studies aimed at evaluating the role of carbohydrates in the selective delivery of whole molecules into cancerous cells.

## Introduction

Cancer is the second-leading cause of death after cardiovascular diseases and was responsible for an estimated 9.6 million deaths in 2018. Globally, about one in six deaths is due to cancer.[1,2] Although several strategies have been developed to fight cancer, killing neoplastic cells without affecting healthy cells is still a challenge.

Within this lively field of research, a wide range of metal-based compounds have been designed and tested in the last decades to achieve the highest antiblastic activity along with a good toxicological profile.[3] To enhance drug selectivity, researchers exploit specific target proteins on the cell's phospholipid bilayer, which are overexpressed in neoplastic cells, by conjugating the drug to the corresponding antibody or small biomolecule.[4–8] In particular, this paper discloses the synthesis and preliminary biological studies of coordination compounds functionalized with monosaccharides to obtain selective delivery of the cytotoxic metal payload into the tumor tissue. Discovered by Warburg in 1924, cancer cells require a larger supply of nutrients, in particular carbohydrates, than healthy cells, due to a series of metabolic mutations.[9–12] Most neoplastic cells therefore overexpress glucose-transporter proteins, in particular those belonging to the GLUT family, in their cell membrane, and this phenomenon is correlated with poor patient prognosis.[13–15]

In recent years, this histopathological behavior was exploited by a few research groups, in particular those of Gao[16–20] and Lippard,[21,22] who conjugated oxaliplatin to functionalized monosaccharides at different positions of the pyranose ring and tested the obtained $Pt^{II}$ complexes for anticancer properties with promising results.

In this work, we combine some $Au^{III}$ and $Cu^{II}$ dithiocarbamates (DTCs) with various carbohydrates. The metal centers $Au^{III}$ and $Cu^{II}$ were chosen owing to their well-known low-micromolar cytotoxic effects, when complexed with DTCs[23,24] or other appropriate ligands,[25,26] against a wide panel of human tumor cell lines. In this regard, different mechanisms of action have been recognized in the literature over the last years: for example, while reactivity toward the selenoenzyme thioredoxin reductase, aquaporins, proteasome, or PARP-1 has been detected for $Au^{III}$ compounds,[27–31] induced oxidative DNA or mitochondrial damage has been observed for $Cu^{II}$ counterparts.[26,32]

DTCs are bidentate anions forming very stable coordination compounds.[33] The strong chelating effect can prevent ligand substitutions, thus favoring the application of this class of complexes for biomedical purposes.

[a] Dr. N. Pettenuzzo, Dr. L. Brustolin, E. Coltri, Dr. C. Nardon, Prof. D. Fregona
Department of Chemical Sciences (DISC), University of Padova, Via Marzolo 1, 35131, Padova (Italy)
E-mail: dolores.fregona@unipd.it

[b] Dr. N. Pettenuzzo, Dr. L. Brustolin
Department of Surgical, Oncological and Gastroenterological Sciences (DISCOG), University of Padova, Via Giustiniani 2, 35128, Padova (Italy)

[c] Dr. A. Gambalunga, Dr. F. Chiara, Prof. A. Trevisan
Department of Cardio-Thoraco-Vascular Sciences and Public Health (DCTV), University of Padova, Via Giustiniani 2, 35128, Padova (Italy)

[d] Dr. B. Biondi
Institute of Biomolecular Chemistry, Padova Unit, CNR, Via Marzolo 1, 35131, Padova (Italy)

Supporting information for this article can be found under: https://doi.org/10.1002/cmdc.201900226.

Concerning the nature of the selected monosaccharide (D-glucose, D-galactose, and D-mannose), D-glucose is the most common in the body and the last two diastereomers show a similar affinity for GLUT proteins.[34–37] Three different DTC ligands were successfully complexed to the $Au^{III}$ or $Cu^{II}$ metal centers. It is worth highlighting that the best method to conjugate the monosaccharide to the dithiocarbamato moiety turned out the glycosylation reaction, discovered by Fisher and optimized during the last century.[38–40]

## Results and Discussion

### Synthesis and characterization of the ligands

The first step of the synthesis of the dithiocarbamato ligands conjugated with D-glucose, D-galactose and D-mannose (Figure 1) is the glycosylation reaction between the corresponding pentaacetylated glycosyl donor and the carboxybenzyl-protected 2-*N*-methylaminoethanol (Cbz-2-*N*-methylaminoethanol) as glycosyl acceptor in dry $CH_2Cl_2$ (Scheme 1).[41] This step undergoes the activating process promoted by the Lewis acid $BF_3{\cdot}Et_2O$.[42] In particular, the role of the Lewis acid is to favor the leaving of the acetyl group at the anomeric carbon atom with the subsequent formation of a carbenium ion.[43,44] Contrary to Fischer's glycosylation, in which unprotected carbohydrates are used, in the case of acetylated sugars the carbonyl oxygen atom of the acetyl group at the C2 position can stabilize the carbenium intermediate. When this stabilizing group is present, the reaction becomes highly stereoselective thanks to the assisted stabilization of the adjacent acetyl group that prevents axial nucleophilic attack of the glycosyl acceptor. In particular, the equatorial substituent at C2 for D-glucose and D-galactose drives the selective formation of β-anomeric products.[41] Conversely, in the case of D-mannose, an α-mannoside is obtained because of the axial position of the acetyl group at C2.[41] Although the reaction is rapid and highly stereoselective, many byproducts are formed in solution due to the reactivity of the carbenium ion, which can interact with other nucleophiles (e.g., water and acetate anion). A very low yield, ranging from 10 to 28%, was recorded in all cases after the glycosylation step. Conversely, the deacetylation and the hydrogenation processes (second and third synthetic steps, respectively) provide the unprotected glycosides almost quantitatively.[41,45] During the process optimization we observed that if column purification is performed only after the second step instead of immediately after the glycosylation reaction, higher yields can be obtained.

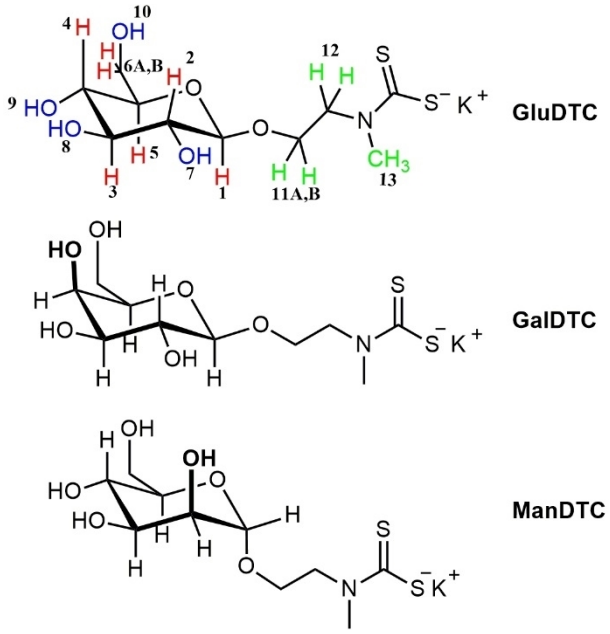


**Figure 1.** Glycoconjugated dithiocarbamato ligands synthesized in this work.

During the dithiocarbamate synthesis (Scheme 1 (iv), Figure 1), we observed that the nucleophilic attack of the glycosyl-conjugated secondary amine toward $CS_2$ in water is slower (6 h) than the same process involving less sterically hindered alkyl amines as starting material (usually 1–2 h, for example, piperidine).[24,33]

All the NMR spectra of the ligands were acquired in [$D_6$]DMSO and are provided in the Supporting Information. This aprotic solvent allows the detection of resonances related to the alcoholic functions of the monosaccharides. Moreover, spectra recorded in [$D_6$]DMSO show better solved peaks in the 2.9–4.9 ppm range. In contrast, acquisitions in $D_2O$ or MeOD are characterized by closer peaks, thus hampering a proper integration process.

The $^1$H NMR spectra of the glycosyl-functionalized ligands are characterized by the presence of several multiplets. Notably, 11 of the 18 total protons (i.e., the methynic protons of the pyranose ring, the methylenic protons of the ethylic spacer, and the methylenic protons at C6 as shown in Figure 1) are diastereotopic, and each of them gives rise to a multiplet in different regions of the spectrum. In this regard, a one-dimensional $^1$H NMR investigation does not provide sufficient information to unambiguously assign every resonance to the corresponding proton set.

Figure 2 (top) shows the 2D $^1$H–$^1$H COSY spectrum of the ligand GluDTC, useful to better attribute each proton within the structure (the corresponding 1D spectrum is shown in Figure 2, at bottom, and the resonances are listed in Table 1). The 2D spectra recorded for the D-galactoside and D-mannoside derivatives are reported in the Supporting Information.

As shown in the 1D $^1$H NMR spectrum of the GluDTC ligand (Figure 2 bottom), the groups of protons in α position with respect to the dithiocarbamato moiety resonate at 3.40 and at about 4.20 ppm for the *N*-methyl and the *N*-methylene protons, respectively. These values are in agreement with data reported for other dithiocarbamates bearing similar substituents surrounding the dithiocarbamic nitrogen atom (for example, the sarcosine-DTC ligand).[46]

The protons of the hydroxy groups of the pyranose ring couple with the adjacent methynic protons and give rise, in the case of GluDTC, to three doublets (protons 7, 8, 9) and a triplet (proton 10), at 4.95, 4.87, 4.83, and 4.50 ppm, respective-

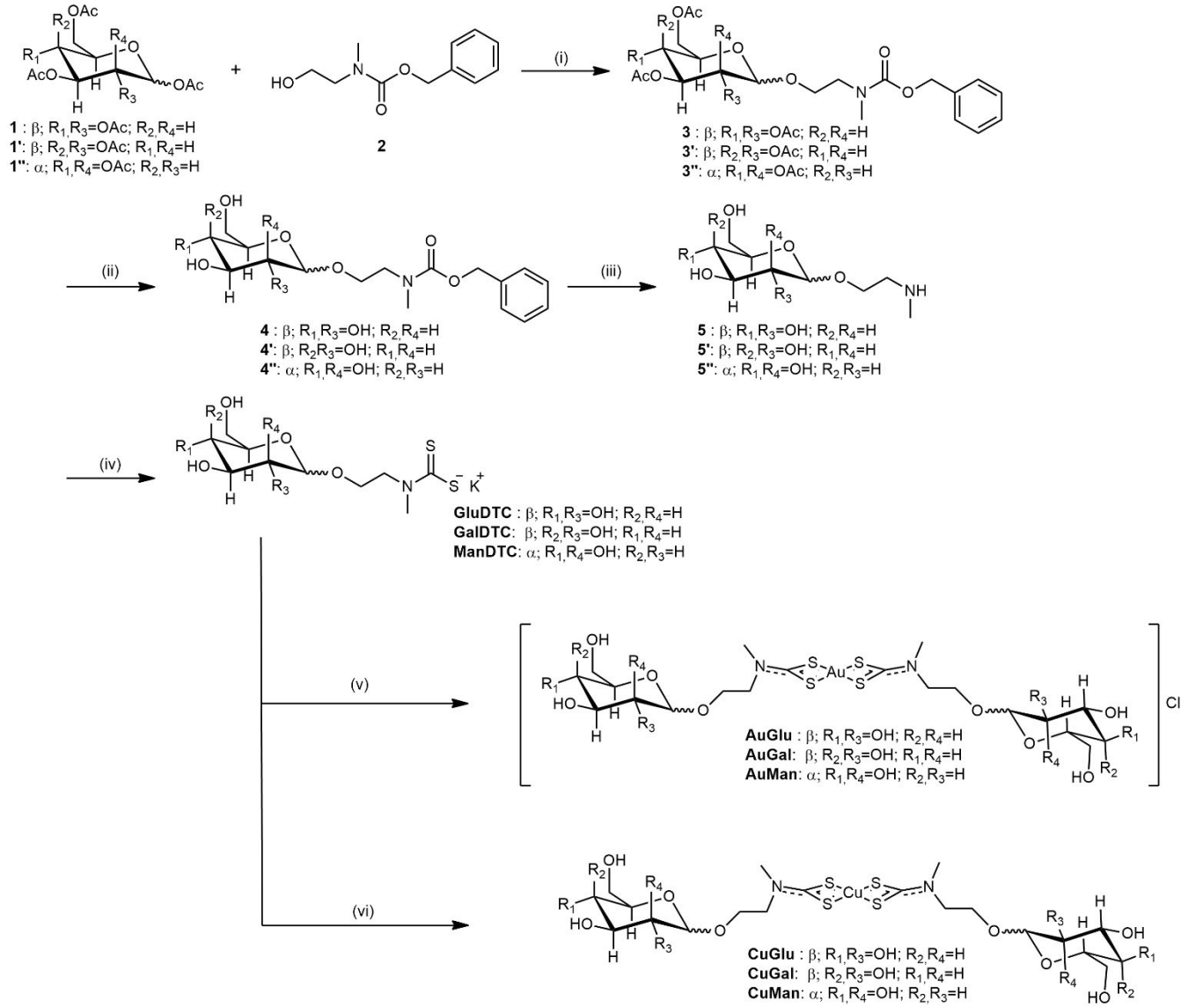


**Scheme 1.** Reagents and conditions: (i) $BF_3{\cdot}Et_2O$, dry $CH_2Cl_2$, 0 °C→RT, 16 h; (ii) NaOMe, MeOH, RT, 16 h, column chromatography; (iii) $H_2$/Pd, MeOH/EtOAc, RT, 2 h; (iv) $CS_2$, KOH, $H_2O$, 0 °C, 6 h, lyophilization; (v) $[Au^{III}(PPh_3)Cl_3]$, $CH_2Cl_2$/MeOH/$H_2O$ (10:10:1 *v/v*), RT (byproducts: $[Au^{I}(PPh_3)Cl]$, $PPh_3{=}O$, KCl, HCl); (vi) $CuCl_2{\cdot}2H_2O$, acetone/MeOH (1:1 *v/v*), RT (byproduct: KCl).

ly (Table 1). Generally, the resonances of the equatorial protons in the pyranose ring are shifted to lower fields relative to the axial protons.[47,48]

In particular, all methynic protons in the β-D-glucoside ligand experience the most shielding effect relative to the axial counterparts of the β-D-galactoside and α-D-mannoside derivatives (except for the $^1H$ at $C_1$). For example, the proton at the position C2 of the former resonates at highest field (2.93 ppm) with a difference of 0.66 ppm with respect to the equatorial proton at the same position of the ManDTC (3.59 ppm). The same is true for the axial proton at C2 of GalDTC relative to the equatorial proton of ManDTC. Likewise, the equatorial C4 proton in GalDTC resonates at lower fields with respect to the corresponding protons of the other derivatives.

The shielding effect occurring for the methynic protons is accompanied by deshielding for the alcoholic protons. In fact, the hydroxylic protons resonate at higher chemical shifts in the case of GluDTC, in which all the hydroxy groups are in an equatorial configuration.

The FTIR spectra of all dithiocarbamato ligands were collected in the medium (4000–600 $cm^{-1}$) wavenumber domain and are reported in the Supporting Information (Figures S3, S6, S9). The diagnostic absorptions are listed in Table 2 and are compared with those of the dimethyl dithiocarbamato molecule, which, similarly to glycoside analogues, bears two linear alkyl substituents in α position with respect to the N–CSS moiety.

Two main IR regions are taken into account when characterizing DTC derivatives, both ligand salts and metal–DTC complexes. First is the spectral region 1100–1550 $cm^{-1}$, in which the $\nu$(N–CSS) band can be found and its position depends strongly on the extent of double bond character of the N–C bond.[24] In the case of a single-bond form, the band is located

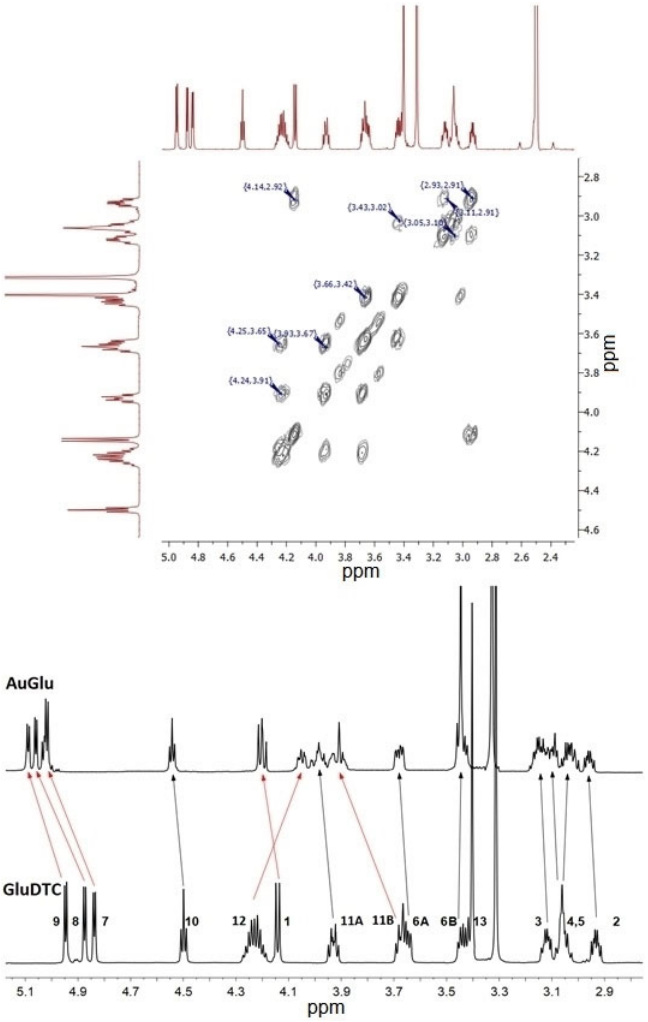


**Figure 2.** Top: COSY 2D $^1$H–$^1$H NMR ([D$_6$]DMSO, 600 MHz, 25 °C) spectrum of GluDTC (*O*-ethyl, *N*-methyl, β-D-glucopyranosyl dithiocarbamato, potassium salt), reported as an example. Bottom: stacked $^1$H NMR spectra of GluDTC and AuGlu. On passing from the free ligand to the complex, the most characteristic deshielding and shielding effects are highlighted with red arrows.

**Table 1.** $^1$H NMR resonances of the synthesized glycosylated DTC ligands in [D$_6$]DMSO at 25 °C.

| Protons[a] | δ [ppm] | | |
|---|---|---|---|
| | GluDTC | GalDTC | ManDTC |
| **1** (C–*H* backbone) | 4.14 (d) | 4.10 (d) | 4.61 (s) |
| **2** (C–*H* backbone) | 2.93 (m) | 3.25 (m) | 3.59 (m) |
| **3** (C–*H* backbone) | 3.11 (m) | 3.25 (m) | 3.30 (m) |
| **4** (C–*H* backbone) | 3.06 (m) | 3.62 (m) | 3.38 (m) |
| **5** (C–*H* backbone) | 3.05 (m) | 3.31 (m) | 3.45 (m) |
| **6** (C–*H* backbone) | 3.65, 3.44 (m) | 3.46–3.52 (m) | 3.63, 3.45 (m) |
| **7** ($C_2$–*OH*) | 4.83 (d) | 4.64 (m) | 4.67 (d) |
| **8** ($C_3$–*OH*) | 4.95 (d) | 4.80 (m) | 4.65 (d) |
| **9** ($C_4$–*OH*) | 4.87 (d) | 4.31 (d) | 4.52 (d) |
| **10** ($C_6$–*OH*) | 4.50 (t) | 4.56 (t) | 4.38 (t) |
| **11** (*O*–$CH_2$ spacer) | 3.93, 3.67 (m) | 3.90, 3.67 (m) | 3.75, 3.63 (m) |
| **12** (*N*–$CH_2$ spacer) | 4.23 (m) | 4.22 (t) | 4.21 (m) |
| **13** (*N*–$CH_3$ spacer) | 3.40 (s) | 3.40 (s) | 3.40 (s) |

[a] Numbered as shown in Figure 1.

**Table 2.** Main IR absorption peaks of the dimethyl dithiocarbamate and the three glycosylated ligands.

| Vibrations[a] | IR [cm$^{-1}$] | | | |
|---|---|---|---|---|
| | Dimethyl DTC–Na$^+$ | GluDTC | GalDTC | ManDTC |
| ν(N–CSS) (s) | 1486 | 1481 | 1481 | 1480 |
| $\nu_{as}$(S–C–S) (m) | 962 | 953 | 952 | 955 |
| $\nu_{as}$(C–O) (s) | – | 1077–1033 | 1077–1043 | 1083–1055 |
| ν(O–C–O) (w) | – | 898 | 892 | 882 |
| ν(C–H sp$^3$) (m) | – | 2926 | 2931-2890 | 2929 |
| δ(C–H sp$^3$) (m) | – | 1424 | 1422 | 1413 |
| | | 1377 | 1377 | 1377 |
| | | | | 1353 |
| ν(C–C) (m) | – | 1286 | 1287 | 1280 |
| | | 1259 | 1258 | 1258 |
| | | 1210 | 1210 | 1210 |
| ν(OH) (br) | – | 3392 | 3365 | 3393 |

[a] s: strong, m: medium, w: weak, and br: broad.

at 1250–1350 cm$^{-1}$, whereas it is found at higher wavenumbers (1640–1690 cm$^{-1}$) if the DTC ligand contains a basically double C=N bond (thioureidic form).[24,49]

The N–CSS band can be recognized at about 1480 cm$^{-1}$ for all the three synthesized ligands, denoting a pronounced double bond character. As a comparison, the same vibrational frequency for the dimethyl dithiocarbamate is at 1486 cm$^{-1}$, pointing out an excellent correlation between the simplest aliphatic ligand and the glycosyl-functionalized ligands.

The band associated with the asymmetric stretching $\nu_a$(CSS), detectable in the region ranging from 800 to 1100 cm$^{-1}$, is found at 952–955 cm$^{-1}$ for the ligands under investigation, with excellent correlation with respect to the same absorption for the dimethyl dithiocarbamate at 962 cm$^{-1}$.[50–52]

Other areas of the spectrum provide valuable information regarding the carbohydrate moiety, in particular the "sugar region" (1200–950 cm$^{-1}$) and the "anomeric region" (950–750 cm$^{-1}$[1]).[53,54]

The overlapping intense bands of C–O and C–C stretching vibrations in glycosidic bonds and pyranosic ring predominate in the former region as shown in Figures S3, S6, S9 and Table 2. In contrast, the "anomeric region" contains weaker bands of more diagnostic skeletal vibrations sensitive to the nature of the substituent in the acetal group and the anomeric structure. In particular, based on published data, *O*-glycosides in β-anomeric form give rise to a weak band related to the O–C–O stretching between 950 and 890 cm$^{-1}$, whereas α-anomers present a similar absorption at lower wavenumbers (from 890 to 750 cm$^{-1}$).[54] These bands are visible in the FTIR spectra of the synthesized ligands, confirming the stereoselectivity of the glycosylation reaction that led to the formation of β-anomers for GluDTC and GalDTC derivatives (ν(OCO) = 898 and 892 cm$^{-1}$), and α-stereoisomers in the case of ManDTC (ν(OCO) = 882 cm$^{-1}$).[54,55] However, the assignment for this vibration mode is not unambiguously determined in literature, as bands for other types of vibrations (not clearly understood) also occur in the same region (Table 3).

**Table 3.** Proton resonances of the glycosylated ligand in the $Au^{III}$ [1:2]Cl complexes in [$D_6$]DMSO at 25 °C.

| Protons[a] | δ [ppm] | | |
|---|---|---|---|
| | AuGlu | AuGal | AuMan |
| **1** (C–*H* backbone) | 4.20 (t) | 4.15 (d) | 4.66 (s) |
| **2** (C–*H* backbone) | 2.94–2.98 (m) | 3.20–3.27 (m) | 3.59 (m) |
| **3** (C–*H* backbone) | 3.09–3.17 (m) | 3.20–3.27 (m) | 3.19–3.22 (m) |
| **4** (C–*H* backbone) | 3.00–3.06 (m) | 3.63 (m) | 3.34–3.38 (m) |
| **5** (C–*H* backbone) | 3.09–3.17 (m) | 3.33–3.37 (m) | 3.43–3.46 (m) |
| **6–7** (C–*H* backbone) | 3.68, 3.43 (m) | 3.48–3.55 (m) | 3.66, 3.43 (m) |
| **8–9** (*O*–$CH_2$ spacer) | 3.88–4.06 (m) | 3.86–4.05 (m) | 3.37–3.97 (m) |
| **10–11**(*N*–$CH_2$ spacer) | 3.88–4.06 (m) | 3.86–4.05 (m) | 4.04, 3.75 (m) |
| **12** (*N*–$CH_3$ spacer) | 3.43 (s) | 3.43 (s) | 3.43 (s) |
| **13** ($C_6$–*OH*) | 4.54 (t) | 4.58 (t) | 4.52 (t) |
| **14** ($C_4$–*OH*) | 5.06 (d) | 4.40 (d) | 4.80–4.82 (m) |
| **15** ($C_3$–*OH*) | 5.09 (d) | 4.90 (d) | 4.65 (d) |
| **16** ($C_2$–*OH*) | 5.01 (d) | 4.76 (d) | 4.80–4.82 (m) |

[a] Numbered as shown in Figure 1.

### Synthesis of bis-dithiocarbamato $Au^{III}$ complexes

After the synthesis and characterization of the three DTC ligands, the next step was the complexation reaction with $Au^{III}$ centers. A total of three $Au^{III}$ complexes were synthesized with a 1:2 metal-to-ligand stoichiometric ratio (hereinafter referred to as [1:2]Cl).

The novel class of dithiocarbamato ligands explored in this study possess four hydroxy groups that can interact with the metal center, obtaining several byproducts. As a consequence, a new synthetic pathway, which permits synthesis of the [1:2]Cl compounds in good purity, was designed and optimized in this work (Scheme 1).[25,56]

The reaction starts from a $CH_2Cl_2$ solution containing the triphenylphosphino trihalo $Au^{III}$ derivative [$Au^{III}PPh_3Cl_3$] as reagent, and the desired product is formed quantitatively upon the addition of one equivalent of dithiocarbamato ligand, dissolved in a methanol/water mixture (10:1 *v/v*) (Scheme 1, (v), Figure S1). From a mechanistic point of view, it is possible to suppose that coordination of the first DTC ligand to the $Au^{III}$ sphere promotes the formation of an instable intermediate of the type $[Au^{III}Cl(DTC)(PPh_3)]^+$. On one hand, the chelation of a second dithiocarbamate leads to the desired product as a chloride salt. On the other, release of the triphenylphosphine is favored by its participation in a redox equilibrium (oxidation to $PPh_3O$) paralleled with the reduction of a second equivalent of the [$Au^{III}Cl_3(PPh_3)$] reagent, forming the stable [$Au^{I}Cl(PPh_3)$] complex.

### Synthesis of bis-dithiocarbamato $Cu^{II}$ complexes

The copper ion in the +2 oxidation state can coordinate two DTC molecules, for instance, by starting from the $CuCl_2{\cdot}2H_2O$ salt, thus letting the chlorides out and yielding a neutral tetracoordinated and more stable product with a 1:2 metal-to-DTC ligand ratio.[51,57]

Examples of $Cu^{II}$ dithiocarbamato compounds with a M/L stoichiometry other than 1:2 have never been reported on the basis of this synthetic route. However, unstable dimeric complexes of the type $[Cu^{II}Cl(DTC)]_2$ with two chlorides as bridging ligands can be obtained by redox reaction between a $Cu^{I}$ precursor and thiuram disulfide in an aprotic solvent.[58] In this research field, Vecchio and co-workers studied the copper(II) behavior in solution in the presence of various Cu/DTC stoichiometries.[59]

All reactions with glycosylated DTCs were carried out in polar solvent by adding the ligands to $CuCl_2{\cdot}2H_2O$ (Scheme 1 (vi)). Due to high hydrophilicity, the purification of the copper(II) derivatives from reaction byproducts, such as KCl and the unreacted ligand, was difficult to achieve. Thus, $C_{18}$ column chromatography followed the synthesis of the complexes.

### Characterization of dithiocarbamato $Au^{III}$ and $Cu^{II}$ complexes

All the obtained compounds were fully characterized by means of $^1$H NMR, FTIR, UV/Vis, ESI-MS and elemental analysis (see Supporting Information for $^1$H NMR and FTIR spectra). The $^1$H NMR spectra of all the $Au^{III}$ complexes (600 MHz, 298 K) were acquired in [$D_6$]DMSO (Supporting Information) comparing their resonances with those of the corresponding ligands (an example is shown in Figure 2, bottom). In particular, upon coordination the protons are generally characterized by downfield shifts caused by the electron-withdrawing effect of the electronegative metal. Only the $H_{12}$ protons of the spacer are affected by a shielding effect of about 0.2 ppm.

Concerning the $Cu^{II}$ derivatives, a general broadening of the resonances is observed when performing NMR analyses. This effect, associated with the paramagnetic nature of the metal center ($d^9$ electronic configuration), appears as hyperfine shift ($\delta$) to NMR signals and the shortening of both nuclear longitudinal ($T_1$) and transverse ($T_2$) relaxation times.[60] The shifts and the signal broadening, observed in particular for the closest protons of the ethylic spacer ($H_{12}$ and $H_{13}$), result in resonances with low intensities overlapping with other peaks of the carbohydrate backbone. Therefore, these spectra (Figure S15 shows an example) proved not so useful for the characterization of the complexes and other diagnostic methods were exploited in this work.

Regarding the FTIR characterization (Table 4), the coordination of the metal center strongly affects the SSC–N stretching frequency, which is upshifted by about 80 and 35 $cm^{-1}$ relative to that of the free ligands in all $Au^{III}$- and $Cu^{II}$-based compounds, respectively. For all three $Cu^{II}$–DTC complexes, a strong band is observed at about 1515 $cm^{-1}$, pointing out a weaker N–CSS bond than that recorded for the Au counterparts.[61,62] For all complexes the CSS stretching mode cannot be clearly evaluated instead, due to the presence of strong bands related to the backbone vibrations which overlap the $\nu_a$(C–S) absorption usually occurring at about 940–1060 $cm^{-1}$.[51,63,64]

Interestingly, all the spectra of the synthesized complexes show a diagnostic absorption at about 890 $cm^{-1}$, recognized as $\nu$(OCO) vibration of the glycosidic linkage. In fact, as de-

**Table 4.** Main IR absorption bands of the $Au^{III}$ complexes and $Cu^{II}$ glycosylated compounds.

| Complex | IR [$cm^{-1}$] | | | | | |
|---|---|---|---|---|---|---|
| | AuGlu | AuGal | AuMan | CuGlu | CuGal | CuMan |
| $\nu$(N–CSS) | 1565 | 1564 | 1564 | 1514 | 1516 | 1516 |
| $\nu_{as}$(C–O) | 1076 | 1072 | 1054 | 1077 | 1072 | 1057 |
| $\nu$(O–C–O) | 897 | 891 | 880 | 897 | 898 | 884 |
| $\nu_s$(CSS) | 554 | 528 | 528 | 565 | 542 | 533 |
| $\nu$(CS) + $\delta$(SCS) | 486 | 480 | 481 | 291 | 267 | 293 |
| $\nu_a$(M–S) | 386 | 386 | 384 | – | – | – |
| $\nu_s$(M–S) | – | – | – | 357 | 352 | 364 |

scribed previously, these bands can be exploited to distinguish between the $\alpha$ and $\beta$ anomers.[54]

Moving to far FTIR, for the $Au^{III}$ compounds the absorption in the range 370–440 $cm^{-1}$ is ascribed to the Au–S asymmetric stretching associated with a bidentate symmetric coordination.[24,52]

The $\nu_s$(M–S) in the copper complexes is set at about 358 $cm^{-1}$, in agreement with published data.[65]

For all the characterized compounds, the vibrational modes related to CSS-ring deformation (combined $\nu$(CS) + $\delta$(SCS) vibrational modes) occur at about 480 $cm^{-1}$ and 280 $cm^{-1}$ for the gold and copper derivatives, respectively.[52,65]

The new dithiocarbamato $Au^{III}$ and $Cu^{II}$ complexes were also characterized by UV/Vis spectrophotometry (see section below about stability in aqueous media and the Supporting Information) as well as by ESI-MS and elemental analysis (see Experimental Section) in order to confirm the expected stoichiometry.

### Log*P* measurements

The lipophilicity of a molecule can be represented as the logarithm of the *n*-octanol/water partition coefficient and often strongly correlates with its pharmacological activity and toxicity.[66] The biphasic solvent system *n*-octanol/water is commonly accepted in the scientific community, as it mimics well the water/phospholipid membrane interface.[67] The results, presented as the mean of at least three independent measurements, are presented in Table 5. Considering the similarity of the three glycosylated ligands, only the values for the *O*-glucosyl derivatives are reported herein as an example. For comparative purposes, the log*P* values of the bis-(piperidine-DTC) $Cu^{II}$ complexes and D-glucose are also listed in Table 5.

**Table 5.** Log*P* values of AuGlu and CuGlu determined at 25 °C by UV/Vis measurements.[a]

| Complex | Log*P* |
|---|---|
| AuGlu | $-1.9 \pm 0.1$ |
| CuGlu | $-1.2 \pm 0.1$ |
| $[Cu(pipeDTC)_2]$[24] | $+1.5 \pm 0.1$ |
| cisplatin $[Pt^{II}(NH_3)_2Cl_2]$[68] | $-2.4$ |
| D-glucose[69] | $-2.82 \pm 0.1$ |

[a] Data are reported as the mean ± SD; each experiment was repeated at least three times. Data for the other reference compounds were obtained from published sources, as indicated.

The negative values found for AuGlu and CuGlu account for the observed high water solubility, and the $Au^{III}$ compounds are more hydrophilic than the copper(II) counterparts. Intriguingly, a difference of log*P* (as absolute value) of 2.7 was detected between the CuGlu and its analogue with piperidine dithiocarbamate as a ligand.

### Stability of the complexes in aqueous media

To determine the stability of the complexes in a medium suitable for biological tests, a sequence of UV/Vis spectra was collected over 72 h after dissolving the synthesized $Au^{III}$ and $Cu^{II}$ derivatives in saline solution (NaCl, 0.9% *w/v*).

The electronic spectra over time of AuGlu and CuGlu, as model compounds, are shown in Figure 3. The spectrum of AuGlu displays two intense bands at 270 nm and 312 nm related to the $\pi^* \leftarrow \pi$ intra-ligand NCS and SCS transitions, similar to 1:2 $Au^{III}$ dithiocarbamato analogues reported in the literature.[52,56,70] Moreover, as chloride salt, it is stable over 72 h under physiological conditions. The UV/Vis spectrum of CuGlu shows different bands. The absorption at 266 nm is ascribable to the overlap between the $\pi^* \leftarrow \pi$ absorption of the conjugated NCSS group and the intra-ligand $\pi^* \leftarrow \pi$ transition located mainly in the CSS moiety.[71,72] Moreover, the broad band at 428 nm is related to the d–d transitions derived from the distorted symmetry ($D_{2h}$ or $C_{2v}$, $\varepsilon = 11930\ L\,mol^{-1}\,cm^{-1}$), the theoretical explanation of which is reported elsewhere.[73]

To sum up, it is important to highlight that all the synthesized complexes show optimal stability in aqueous solution over 72 h, as no substantial variations of the main bands are detectable for each of them (see Supporting Information Figures S31–S34 for the UV/Vis spectra over time of the $Au^{III}$- and $Cu^{II}$-galactosyl and mannosyl derivatives). However, an intracellular dissociation of the complexes cannot be excluded.[74]

### In vitro cytotoxic activity evaluation

To identify the best compound for future studies, all synthesized complexes and the reference drug cisplatin were tested against the HCT116 human colorectal carcinoma cell line, and the results are summarized in Table S1. The new water-soluble $Au^{III}$ complexes are inactive, with $IC_{50}$ values higher than 50 μM. On the other hand, the CuGlu complex shows cytotoxic activity at low micromolar concentrations, in contrast to the CuGal and CuMan derivatives.

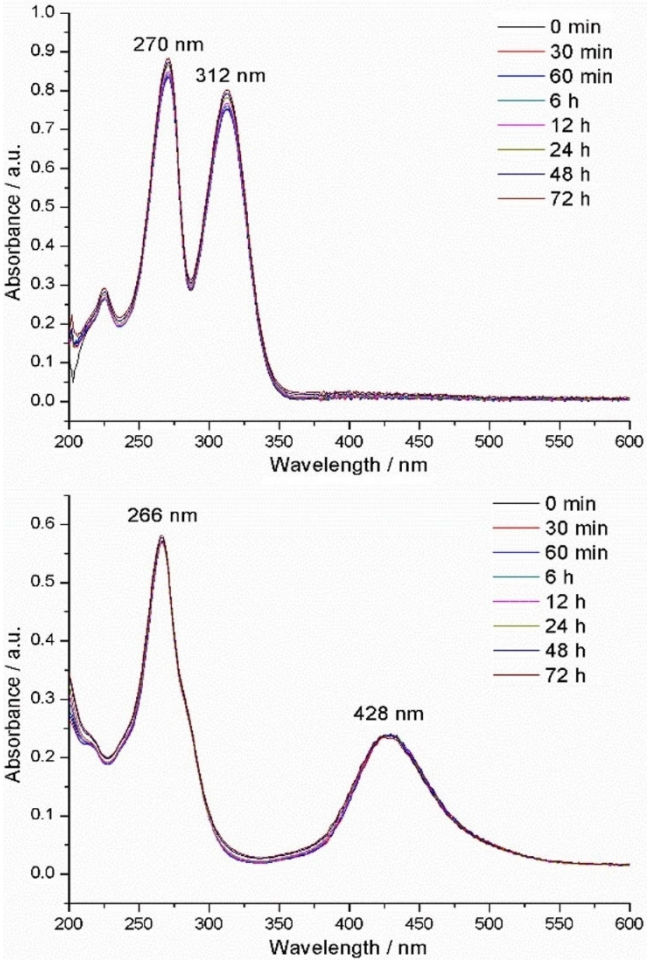


**Figure 3.** UV/Vis analysis of AuGlu (top, 30 μM) and CuGlu (bottom, 20 μM) dissolved in saline solution at 25 °C over 72 h.

Scientific evidence suggests that HCT116 neoplastic cells overexpress GLUT-1 in their phospholipid bilayer.[75] The collected results indicate that the $Au^{III}$ complexes, CuGal and CuMan, are not good substrates for glucose transporter proteins. Moreover, cell uptake through the phospholipid bilayer via passive transport is unlikely due to their high hydrophilicity and the ionic nature of the gold-based compounds.

Afterward, to check whether CuGlu ([$Cu^{II}$(DTC-β-D-glucose)$_2$]) can selectively target one or more glucose transporters, HCT116 cells were exposed for 72 h to two different GLUT inhibitors, being added together with CuGlu to the cell culture medium in selected wells. The first is *O*-ethylidene-α-D-glucose (EDG), used as a GLUT-1 inhibitor at a concentration of 10 mM,[22,76] and the second is phlorizin dihydrate, which irreversibly binds the active site of SGLT (sodium-dependent glucose co-transporter) proteins at 1 mM.[16,77] Furthermore, to evaluate the competitiveness of CuGlu (as potential GLUT substrate) with other carbohydrates, D-glucose was selected as competitor and added to the medium at a concentration of 50 mM in the presence of CuGlu. The results of the mitochondrial viability tests in the presence of the inhibitors and competitor are listed in Table 6.

**Table 6.** Cytotoxicity values of the CuGlu complex toward HCT116 cancer cells, alone or in the presence of a GLUT1 or SGLT inhibitor, or a competitor (D-glucose).

| Complex | $IC_{50}$ [μM][a] | | | |
|---|---|---|---|---|
| | DMEM[b] | Phlorizin[c] | EDG[d] | D-Glucose[e] |
| CuGlu | 2.7 ± 0.4 | 2.6 ± 0.2 | 2.1 ± 0.2 | 2.0 ± 0.1 |

[a] Determined at 72 h, 8000 cells per well. Data are reported as the mean ± SD; each experiment was repeated at least three times, and each concentration tested in at least three replicates. [b] CuGlu alone; in low-glucose DMEM. [c] SGLT inhibitor, present at 1 mM. [d] GLUT1 inhibitor, present at 10 mM. [e] Competitor, present at 50 mM.

The data highlight no remarkable change of the antiproliferative activity after the addition of the two inhibitors or the competitor, in contrast to what was observed for similar metallodrugs by Gao and co-workers, who studied a new class of oxaliplatin-based sugar monoconjugates.[16] The observed behavior could be associated with the presence of two hydrophilic carbohydrate units per anticancer Cu-based molecule.

## Conclusions

Compared with the work of Vecchio and collaborators,[59] wherein the authors studied $Cu^{II}$ complexation by a series of glucosylated DTC ligands in solution, in this study a new class of dithiocarbamato complexes containing a carbohydrate moiety as cancer-targeting agent were disclosed. After the design phase, all the compounds were synthesized, characterized and tested in vitro as potential metallodrugs. In particular, the synthetic conditions were optimized for three different monosaccharides, and the desired complexes were obtained in good yield and purity. The compounds involve two sugar units linked through bulky alkyl amines, but, from a biological point of view, the first experiments highlighted no targeting effect of the carbohydrate functionalization.

Among all, the CuGlu compound showed an interesting $IC_{50}$ value toward the HCT116 human colorectal carcinoma cell line. Remarkably, the copper complexes CuGal and CuMan, bearing two diastereomers of D-glucose, do not show any cytotoxic properties. The next step will be in vivo evaluations of the role of the carbohydrate to further determine whether active transport is involved in the mechanism of action of the CuGlu complex.

## Experimental Section

**General experimental methods**: All reagents and solvents for the syntheses were purchased from commercial sources and used as received. Elemental analyses were carried out at the microanalysis laboratory (Chemistry Department, University of Padova) with a Carlo Erba 1108 CHNS-O micro-analyzer. ESI-MS spectra were recorded on a Mariner Perspective Biosystem instrument, setting a 5 kV ionization potential and a 20 μL $min^{-1}$ flow rate. A mixture of coumarin and 6-methyltryptophan was used as a standard in positive ionization mode. Samples were dissolved in methanol, and the same solvent was used as eluent. ESI-MS spectra were processed

by Data Explorer software. Infrared spectra were recorded at room temperature under $N_2$ atmosphere, in solid KBr by a spectrophotometer Nicolet Nexus 5SXC instrument in the range 4000–400 $cm^{-1}$ (32 scansions, 2 $cm^{-1}$ resolution) and in Nujol between two polyethylene tablets by a spectrophotometer Nicolet Nexus 870 in the range 600–50 $cm^{-1}$ (200 scansions, 4 $cm^{-1}$ resolution). $^1$H NMR one-dimensional spectra were recorded in $CDCl_3$, [$D_4$]MeOH, or [$D_6$]DMSO at 298 K on a Bruker Avance DMX 600 spectrometer equipped with a TXI-5 mm *x,y,z*-field gradient probehead, with Topspin 1.3 software package, operating in Fourier transform. Typical acquisition parameters ($^1$H: 600.13 MHz): 128 transients (for bidimensional acquisition: 512 transients of 32 scans/block), spectral width 7.5 kHz, 2 k data points and a delay time of 7.0 s. Chemical shifts were referred to solvent peak. Peak multiplicity is described as follows: s (singlet), d (doublet), dd (doublet of doublets), ddd (doublet of doublets of doublets), t (triplet) and m (multiplet). For the synthesis of fully acetylated β-D-glucose **1** and β-D-galactose **1′**, the same procedure as that reported by Yamada and co-workers was carried out.[78]

**Penta-*O*-acetyl D-mannopyranoside (1″)**: Dry pyridine (50 mL) and acetic anhydride (40 mL) were added to D-mannose (30 mmol) in a 100 mL round-bottom flask. The mixture was kept at RT for four days. In the meantime, the carbohydrate slowly went into solution. Then, the mixture was diluted with EtOAc (100 mL) and transferred into a separatory funnel. At this point deionized water (50 mL) was added, the organic fraction was separated and successively washed three times with deionized water (50 mL), 1 M $HCl_{(aq)}$ (3× 25 mL), saturated aqueous $NaHCO_3$ (3×25 mL) and with an aqueous 5% *w/v* solution of $CuSO_4$ (5×25 mL) to remove excess pyridine from the organic layer. All the obtained organic fractions were combined, dried, and the solvent was evaporated obtaining a clear viscous oil. In one circumstance, white crystalline needles of the pure product were obtained by triturating the syrup with diethyl ether and cooling. Yield: 86%. $^1$H NMR (600 MHz, $CDCl_3$, mixture of anomers): signals of β-anomer: $\delta = 1.98$ (s, 3H), 2.07 (s, 3H), 2.08 (s, 3H), 2.15 (s, 3H), 2.19 (s, 3H), 3.99–4.05 (m, 1H), 4.07 (dd, 1H), 4.26 (dd, 1H), 5.23 (dd, 1H), 5.31–5.34 (m, 2H), 6.06 ppm (d, 1H); signals of α-anomer: $\delta = 1.98$ (s, 3H), 2.03 (s, 3H), 2.07 (s, 3H), 2.15 (s, 3H), 2.16 (s, 3H), 3.79 (ddd, 1H), 4.11 (dd, 1H), 4.28 (dd, 1H), 5.11 (dd, 1H), 5.27 (t, 1H), 5.46 (dd, 1H), 5.84 ppm (d, 1H).

**Benzyl (2-hydroxyethyl-*N*-methyl)carbamate (2)**: To an ice-cold freshly distilled dichloromethane solution (100 mL) containing 2-(*N*-methylamino)ethanol (1 mmol) was added, portion-wise and under stirring, *N*-benzyloxy carbonyloxysuccinimide (Cbz-OSu, 2 mmol) and triethylamine (2 mmol). Two hours later, the mixture was warmed at room temperature and left under vigorous stirring for 72 h. After the completion of the reaction (monitored with TLC by means of ninhydrin colorimetric detection), the solution was diluted with deionized water (50 mL) and transferred to a separatory funnel. The organic fraction was separated and successively washed with $HCl_{(aq)}$ 1 N (3×25 mL), $NaHCO_3$ (sat) (3×25 mL) and brine (2×25 mL). The combined organic fractions were dried with $Na_2SO_4$, filtered and the solvent evaporated, obtaining a crude mixture in the form of viscous oil. The product was then re-dissolved in EtOAc and purified by means of flash column chromatography on silica gel (eluent: EtOAc/ligroin, 7:3 *v/v*, $R_f$: 0.26). The pure product was isolated as a clear oil. Yield: 85%. $^1$H NMR ($CDCl_3$, 600 MHz): $\delta = 2.99$ (s, 3H, $CH_3$), 3.43 (m, 2H, $CH_2OH$), 3.54 (br, 1H, O*H*), 3.72 (m, 2H, $CH_2N$), 5.13 (s, 2H, $CH_2Ph$), 7.35 ppm (m, 5H, Ph).

**General procedure for *O*-glycosylation (3, 3′, 3″)**: To a cold, freshly distilled dichloromethane solution (70 mL) containing fully acetylated carbohydrate (1.0 mmol) and benzyl (2-hydroxyethyl-*N*-methyl)carbamate (1.2 mmol), $BF_3{\cdot}Et_2O$ (5.0 mmol) was added dropwise under stirring in inert atmosphere. The clear yellow mixture was maintained at 0 °C for 1 h and overnight at RT. Then, the solution was firstly neutralized by the dropwise addition of saturated aqueous $NaHCO_3$, transferred to a separatory funnel and then washed with $NaHCO_3$ (2×30 mL), $HCl_{(aq)}$ 1 N (3×30 mL) and brine (3× 30 mL). The combined organic fractions were dried with $Na_2SO_4$, filtered and the solvent removed by rotatory evaporation, obtaining a yellow oil that was used in the next step without further purification.

**General procedure for deacetylation (4, 4′, 4″)**: The syrupy residue obtained in the previous step was dissolved in dry MeOH (20 mL), transferred in a 50 mL round-bottom flask, and excess NaOMe was added at RT. The solution was then kept under inert atmosphere overnight. After completion of the reaction as monitored by TLC, the mixture was neutralized with Amberlite IR-120 $H^+$ resin, filtered, and dried in rotatory evaporator to obtain a yellow oil. The crude product was then re-dissolved in EtOAc, the solution was filtered, and the pure glycosylated product was purified by means of flash column chromatography on silica, obtaining a clear oil (eluent gradient: EtOAc 100%, then EtOAc/MeOH 85:15).

**General procedure for Cbz cleavage**: The deacetylated glycoside was dissolved in EtOAc/MeOH mixture (2:1, 30 mL). Successively, $H_2$ was bubbled in the presence of Pd/C (10% *w/w*) for 2 h under stirring in a 50 mL round-bottom flask equipped with a gas bubbler. The reaction was monitored by means of TLC using an ethanol solution of ninhydrin for the colorimetric detection of the amine. After completion, the mixture was filtered over a pad of Celite, and the solvent was evaporated to dryness, obtaining a clear oil that solidified in a fluffy white solid when dried by vacuum pump.

**2-(*N*-methylamino)ethyl-β-D-glucopyranoside (5)**: Yield: 25%; $^1$H NMR (600 MHz, MeOD): $\delta = 2.36$ (s, 3H, $CH_3$), 2.84–2.86 (m, 2H, $CH_2NH$), 3.15 (dd, 1H, C2-*H*), 3.21–3.24 (m, 2H, C4-*H*, C5-*H*), 3.31 (dd, 1H, C3-*H*), 3.58–3.63 (m, 2H, C6-$H_A$, $CH_AH_BCH_2NH$), 3.81 (dd, 1H, C6-$H_B$), 3.88 (ddd, 1H, $CH_AH_BCH_2NH$), 4.22 ppm (d, 1H, C1-*H*); elemental analysis calcd (%) for $C_9H_{19}NO_6$ (MW = 237.25 g $mol^{-1}$): C 45.56, H 8.07, N 5.90, found: C 44.77, H 8.70, N 5.55.

**2-(*N*-methylamino)ethyl-β-D-galactopyranoside (5′)**: Yield: 28%; $^1$H NMR (600 MHz, MeOD): $\delta = 2.36$ (s, 3H, $CH_3$), 2.80 (ddd, 1H, $CH_2NH$), 2.84 (ddd, 1H, $CH_2NH$), 3.45 (dd, 1H, C3-*H*), 3.49 (ddd, 1H, C5-*H*), 3.52 (dd, 1H, C2-*H*), 3.61 (ddd, 1H, $CH_AH_BCH_2NH$), 3.69 (dd, 1H, C6-$H_A$), 3.73 (dd, 1H, C6-$H_B$), 3.80 (dd, 1H, C4-*H*), 3.91 (ddd, 1H, $CH_AH_BCH_2NH$), 4.21 ppm (d, 1H, C1-*H*); elemental analysis calcd (%) for $C_9H_{19}NO_6$ (MW = 237.25 g $mol^{-1}$): C 45.56, H 8.07, N 5.90, found: C 45.30, H 8.62, N 5.81.

**2-(*N*-methylamino)ethyl-α-D-mannopyranoside (5″)**: Yield: 22%; $^1$H NMR (600 MHz, MeOD): $\delta = 2.36$ (s, 3H, $CH_3$), 2.82–2.86 (m, 2H, $CH_2NH$), 3.48 (ddd, 1H, $CH_AH_BCH_2NH$), 3.56 (ddd, 1H, C5-*H*), 3.63 (t, 1H, C4-*H*), 3.73 (dd, 1H, C6-$H_A$), 3.74 (dd, 1H, C3-*H*), 3.79 (ddd, 1H, $CH_AH_BCH_2NH$), 3.86 (dd, 1H, C2-*H*), 3.86 (dd, 1H, C6-$H_B$), 4.80 ppm (d, 1H, C1-*H*); elemental analysis calcd (%) for $C_9H_{19}NO_6$ (MW = 237.25 g $mol^{-1}$): C 45.56, H 8.07, N 5.90, found: C 45.20, H 8.25, N 5.34.

**General procedure for the synthesis of the glycosylated dithiocarbamato salt**: To a cold aqueous solution (10 mL) containing the free amine (0.5 mmol), was added KOH (1 equiv), followed by excess $CS_2$. After 6 h of stirring, Ar was bubbled for a few minutes to eliminate the excess carbon disulfide still present. Then, the solution was frozen in an $CO_{2(s)}$/acetone bath and lyophilized, leading

to the formation of a yellow viscous oil. The oil was re-dissolved in anhydrous methanol and precipitated with diethyl ether to obtain a white flocculent solid that was collected and dried. The product, as potassium salt, is not hygroscopic and stable for several days at RT.

**Potassium methyl-(2-(β-D-glucopyranosyl)ethyl) dithiocarbamate (GluDTC)**: Yield: 65%; $^1$H NMR ([D$_6$]DMSO, 600 MHz): $\delta$ = 2.93 (m, 1H, C2-*H*), 3.05 (m, 2H, C4-*H*, C5-*H*), 3.11 (m, 1H, C3-*H*), 3.40 (s, 3H, *N*-C*H*$_3$), 3.44, 3.65 (m, 2H, C6-*H*$_{A\text{-}B}$), 3.67, 3.93 (m, 2H, O-C*H*$_2$), 4.14 (d, 1H, C1-*H*), 4.20–4.26 (m, 2H, *N*-C*H*$_2$), 4.50 (t, 1H, C6-O*H*), 4.87 (d, 1H, C4-O*H*), 4.83 (d, 1H, C2-O*H*), 4.95 ppm (d, 1H, C3-O*H*); medium FTIR (KBr): $\tilde{\nu}$ = 2926 ($\nu_a$, C–H), 1481 ($\nu_a$, N–CSS), 953 ($\nu_a$, CSS), 898 cm$^{-1}$ ($\nu$, OCO); ESI-MS *m/z*: [2*M*]$^-$ 623.11 (623.12), [DTC-CS$_2$]$^-$ 236.11 (236.11), [*M*−CH$_2$OH]$^-$ 282.12 (282.05); elemental analysis calcd (%) for C$_{10}$H$_{18}$KNO$_6$S$_2$ (MW = 351.48 g mol$^{-1}$): C 34.17, H 5.16, N 3.99, S 18.25, found: C 33.83, H 5.57, N 3.90, S 17.94.

**Potassium methyl-(2-(β-D-galactopyranosyl)ethyl)dithiocarbamate (GalDTC)**: Yield: 61%; $^1$H NMR ([D$_6$]DMSO, 600 MHz): $\delta$ = 3.25 (m, 2H, C2-*H*, C3-*H*), 3.31 (m, 1H, C5-*H*), 3.40 (s, 3H, *N*-C*H*$_3$), 3.49 (m, 2H, C6-*H*$_{A\text{-}B}$), 3.62 (m, 1H, C4-*H*), 3.67, 3.90 (m, 2H, O-C*H*$_2$), 4.10 (d, 1H, C1-*H*), 4.21–4.24 (m, 2H, *N*-C*H*$_2$), 4.31 (d, 1H, C4-O*H*), 4.56 (t, 1H, C6-O*H*), 4.64 (d, 1H, C3-O*H*), 4.80 ppm (d, 1H, C2-O*H*); medium FTIR (KBr): $\tilde{\nu}$ = 2931–2890 ($\nu_a$, C–H), 1481 ($\nu_a$, N–CSS), 952 ($\nu_a$, CSS), 892 cm$^{-1}$ ($\nu$, OCO), ESI-MS *m/z*: [2*M*]$^-$ 623.11 (623.12), [DTC-CS$_2$]$^-$ 236.11 (236.11), [*M*−CH$_2$OH]$^-$ 282.12 (282.05); elemental analysis calcd (%) for C$_{10}$H$_{18}$KNO$_6$S$_2$ (MW = 351.48 g mol$^{-1}$): C 34.17, H 5.16, N 3.99, S 18.25, found: C 32.04, H 6.55, N 2.98, S 18.55.

**Potassium methyl-(2-(α-D-mannopyranosyl)ethyl)dithiocarbamate (ManDTC)**: Yield: 74%; $^1$H NMR ([D$_6$]DMSO, 600 MHz): $\delta$ = 3.30 (m, 1H, C3-*H*), 3.38 (m, 2H, C4-*H*), 3.40 (s, 3H, *N*-C*H*$_3$), 3.45 (m, 1H, C5-*H*), 3.45, 3.63 (m, 2H, C6-*H*$_{A\text{-}B}$), 3.63, 3.75 (m, 2H, O-C*H*$_2$), 4.16–4.26 (m, 2H, *N*-C*H*$_2$), 4.38 (t, 1H, C6-O*H*), 4.52 (d, 1H, C4-O*H*), 4.61 (d, 1H, C1-*H*), 4.65 (d, 1H, C3-O*H*), 4.67 ppm (d, 1H, C2-O*H*); medium FTIR (KBr): $\tilde{\nu}$ = 2929 ($\nu_a$, C–H), 1480 ($\nu_a$, N–CSS), 955 ($\nu_a$, CSS), 882 cm$^{-1}$ ($\nu$, OCO); ESI-MS *m/z*: [2*M*]$^-$ 623.11 (623.12), [DTC-CS$_2$]$^-$ 236.11 (236.11); elemental analysis calcd (%) for C$_{10}$H$_{18}$KNO$_6$S$_2$ (MW = 351.48 g mol$^{-1}$): C 34.17, H 5.16, N 3.99, S 18.25, found: C 33.69, H 5.40, N 3.97, S 18.52.

**[Au(PPh$_3$)Cl$_3$] (6)**: [Au$^{I}$(PPh$_3$)Cl] (1 mmol), prepared as reported elsewhere,[79] were dissolved in CH$_2$Cl$_2$ (15 mL) in a 50 mL two-necked round-bottom flask, equipped with a rubber septum. At this point, excess chlorine gas was bubbled through a rubber cannula. The mixture, initially colorless, gradually turned bright green–yellow, denoting the formation of related Au$^{III}$ complex [Au$^{III}$(PPh$_3$)X$_3$] in solution.[80] After monitoring the completion of the reaction by TLC, the chlorine flow was then stopped, and Ar was bubbled through for 10 min to remove excess halogen. The complex was not isolated and was used directly within a few minutes.

**General procedure for the synthesis of Au$^{III}$ bis-dithiocarbamato chloride complexes**: To a 50 mL round-bottom flask containing a dichloromethane solution of [Au$^{III}$(PPh$_3$)X$_3$] (0.1 M, 10 mL) was added the glycoconjugated DTC ligand (1 mmol), previously dissolved in a MeOH/H$_2$O mixture (10:1 *v/v*, 11 mL), at room temperature. The immediately formed yellow solid was filtered, washed with dichloromethane (5×10 mL) and dried in vacuum pump in the presence of P$_4$O$_{10}$. Then the product was transferred into a 25 mL round-bottom flask, re-dissolved in cold dry MeOH, to separate the residual KCl by filtration, and precipitated with diethyl ether, obtaining a yellow flocculent solid. This last step was repeated several times until no more KCl was observed at the bottom of the flask after the re-dissolution of the complex in dry methanol. All the three products were soluble in H$_2$O, MeOH, and DMSO.

**Bis(methyl-(2-(β-D-glucopyranosyl)ethyl)dithiocarbamato)gold(III) chloride (AuGlu)**: Yield: 75%; mp: 60 °C; $^1$H NMR ([D$_6$]DMSO, 600 MHz): $\delta$ = 4.20 (d, 1H), 2.94–2.98 (m, 1H), 3.09–3.17 (m, 1H), 3.00–3.06 (m, 1H), 3.09–3.17 (m, 1H), 3.68 (m, 1H), 3.43 (m, 1H), 3.88–4.06 (m, 2H), 3.88–4.06 (m, 2H), 3.43 (s, 3H), 4.54 (t, 1H), 5.06 (d, 1H), 5.09 (d, 1H), 5.01 ppm (d, 1H); medium FTIR (KBr): $\tilde{\nu}$ = 1565 ($\nu_a$, N–CSS), 1076 ($\nu_a$, CO), 987 ($\nu_a$, CSS), 897 cm$^{-1}$ ($\nu$, OCO), far FTIR (Nujol): $\tilde{\nu}$ = 554 ($\nu_s$, CSS), 486 ($\nu_a$, Au-S), 386 cm$^{-1}$ ($\nu_s$, Au-S); ESI-MS *m/z*: [*M*−Cl]$^+$ 821.09 (821.08), [**5**+H]$^+$ 238.14 (238.13); elemental analysis calcd (%) for C$_{20}$H$_{36}$AuClN$_2$O$_{12}$S$_4$ (MW = 857.19 g mol$^{-1}$): C 28.02, H 4.23, N 3.37, S 14.96, found: C 28.16, H 4.31, N 3.22, S 14.90.

**Bis(methyl-(2-(β-D-galactopyranosyl)ethyl)dithiocarbamato)gold(III) chloride (AuGal)**: Yield: 71%; mp: 60 °C; $^1$H NMR ([D$_6$]DMSO, 600 MHz): $\delta$ = 4.15 (d, 1H), 3.20–3.27 (m, 1H), 3.20–3.27 (m, 1H), 3.63 (m, 1H), 3.33–3.37 (m, 1H), 3.48–3.55 (m, 2H), 3.86–4.05 (m, 2H), 3.86–4.05 (m, 2H), 3.43 (s, 3H), 4.58 (t, 1H), 4.40 (d, 1H), 4.90 (d, 1H), 4.76 ppm (d, 1H); medium FTIR (KBr): $\tilde{\nu}$ = 1564 ($\nu_a$, N–CSS), 1072 ($\nu_a$, CO), 954 ($\nu_a$, CSS), 891 ($\nu$, OCO), far FTIR (Nujol): $\tilde{\nu}$ = 528 ($\nu_s$, CSS), 480 ($\nu_a$, Au-S), 386 cm$^{-1}$ ($\nu_s$, Au-S); ESI-MS *m/z*: [*M*−Cl]$^+$ 821.09 (821.08), [**5**′+H]$^+$ 238.13 (238.13); elemental analysis calcd (%) for C$_{20}$H$_{36}$AuClN$_2$O$_{12}$S$_4$ (MW = 857.19 g mol$^{-1}$): C 28.02, H 4.23, N 3.37, S 14.96, found: C 27.97, H 4.10, N 3.31, S 14.51.

**Bis(methyl-(2-(α-D-mannopyranosyl)ethyl)dithiocarbamato)gold(III) chloride (AuMan)**: Yield: 70%; mp: >50 °C; $^1$H NMR ([D$_6$]DMSO, 600 MHz): $\delta$ = 4.66 (d, 1H), 3.59 (m, 1H), 3.19–3.22 (m, 1H), 3.34–3.38 (m, 1H), 3.43–3.46 (m, 1H), 3.66 (m, 1H), 3.43 (m, 1H), 3.37–3.97 (m, 2H), 3.75 (m, 1H), 4.04 (m, 1H), 3.43 (s, 3H), 4.52 (t, 1H), 4.80–4.82 (d, 1H), 4.65 (d, 1H), 4.80–4.82 ppm (d, 1H); medium FTIR (KBr): $\tilde{\nu}$ = 1564 ($\nu_a$, N–CSS), 1054 ($\nu_a$, CO), 973 ($\nu_a$, CSS), 880 cm$^{-1}$ ($\nu$, OCO), far FTIR (Nujol): $\tilde{\nu}$ = 528 ($\nu_s$, CSS), 481 ($\nu_a$, Au-S), 384 cm$^{-1}$ ($\nu_s$, Au-S); ESI-MS *m/z*, [*M*−Cl]$^+$ found (calc.): 821.09 (821.08); elemental analysis calcd (%) for C$_{20}$H$_{36}$AuClN$_2$O$_{12}$S$_4$ (MW = 857.19 g mol$^{-1}$): C 28.02, H 4.23, N 3.37, S 14.96, found: C 28.12, H 3.98, N 3.19, S 15.04.

**General procedure for the synthesis of Cu$^{II}$ bis-dithiocarbamato complexes**: In a 50 mL round-bottom flask CuCl$_2$·2H$_2$O (0.25 mmol) was dissolved in acetone (15 mL) under stirring. At this point, the glycosylated dithiocarbamato ligand as potassium salt (0.5 mmol), previously dissolved in dry MeOH (15 mL), were added dropwise to the light-green acetone solution. The mixture initially turned darker, due to the coordination between excess Cu$^{II}$ ions with the hydroxy groups of the ligand, and then brown, with a small amount of a clear precipitate (KCl). The solution was filtered, the solvent volume decreased by half by rotatory evaporation and a brown flocculent solid was collected after precipitation with diethyl ether. Then, the product was re-dissolved in Milli-Q H$_2$O and purified by reversed-phase column chromatography on C$_{18}$-functionalized silica (eluent H$_2$O-CH$_3$CN, with a gradient from 9:1 to 8:2 in 20 min with 0.05% TFA), obtaining a brown amorphous powder after the lyophilization step. All the three products were soluble in water, DMSO, MeOH and slightly in EtOH.

**Bis(methyl-(2-(β-D-glucopyranosyl)ethyl)dithiocarbamato)copper(II) (CuGlu)**: Yield: 61%; mp: 156 °C (dec.); medium FTIR (KBr): $\tilde{\nu}$ = 1514 ($\nu_a$, N–CSS), 1077 ($\nu_a$, CO), 990 ($\nu_a$, CSS), 897 cm$^{-1}$ ($\nu$, OCO), far FTIR (Nujol): $\tilde{\nu}$ = 565 ($\nu_s$, CSS), 357 ($\nu_a$, Cu-S), 291 cm$^{-1}$ ($\nu_s$, Cu-S); ESI-MS *m/z*: [*M*]$^+$ 687.05 (687.04), [**5**+H]$^+$ 238.14 (238.13); elemental analysis calcd (%) for C$_{20}$H$_{36}$Cu$_2$N$_2$O$_{12}$S$_4$ (MW = 688.31 g mol$^{-1}$): C 34.90, H 5.27, N 4.07, S 18.63, found: C 34.08, H 5.25, N 3.64, S 18.42.

**Bis(methyl-(2-(β-D-galactopyranosyl)ethyl)dithiocarbamato) copper(II) (CuGal)**: Yield: 80%; mp: 147 °C (dec.); medium FTIR (KBr): $\tilde{\nu}$ = 1516 ($\nu_a$, N–CSS), 1072 ($\nu_a$, CO), 960 ($\nu_a$, CSS), 898 $cm^{-1}$ ($\nu$, OCO), far FTIR (Nujol): $\tilde{\nu}$ = 542 ($\nu_s$, CSS), 360 ($\nu_a$, Cu-S), 290 $cm^{-1}$ ($\nu_s$, Cu-S); ESI-MS *m/z*: $[M]^+$ 687.05 (687.04), $[\mathbf{5}'+H]^+$ 238.14 (238.13); elemental analysis calcd (%) for $C_{20}H_{36}Cu_2N_2O_{12}S_4$ (MW = 688.31 g $mol^{-1}$): C 34.90, H 5.27, N 4.07, S 18.63. Found: C 34.50, H 5.21, N 3.22, S 18.48.

**Bis(methyl-(2-(α-D-mannopyranosyl)ethyl)dithiocarbamato) copper(II) (CuMan)**: Yield: 88%; mp: 193 °C (dec.); medium FTIR (KBr): $\tilde{\nu}$ = 1516 ($\nu_a$, N–CSS), 1057 ($\nu_a$, CO), 960 ($\nu_a$, CSS), 884 $cm^{-1}$ ($\nu$, OCO), far FTIR (Nujol): $\tilde{\nu}$ = 533 ($\nu_s$, CSS), 364 ($\nu_a$, Cu-S), 293 $cm^{-1}$ ($\nu_s$, Cu-S); ESI-MS *m/z*: $[M]^+$ 687.04 (687.04), $[\mathbf{5}''+H]^+$ 238.14 (238.13); elemental analysis calcd (%) for $C_{20}H_{36}Cu_2N_2O_{12}S_4$ (MW = 688.31 g $mol^{-1}$): C 34.90, H 5.27, N 4.07, S 18.63, found: C 34.64, H 5.25, N 3.63, S 18.11.

**Log*P* measurements**: The measurements were carried out by UV/Vis techniques recording the electronic spectra of the aqueous solution of the desired compound before ($C_0$) and after mixing it with a pre-saturated octanol solution for 2 h ($C_1$) at RT. The evaluation of the corresponding *n*-octanol/water partition coefficient was carried out exploiting the following equation, using the absorbance value at the maximum absorption wavelength of the spectrum [Eq. (1)]:

$$logP = log\frac{C_{octanol}}{C_{water}} = log\frac{C_0 - C_1}{C_0} \quad (1)$$

**In vitro viability studies**: HCT116 cells (American Type Culture Collection, ATCC) were cultured in 75 $cm^2$ cell culture flasks in low-glucose Dulbecco's modified Eagle's medium (LG-DMEM), with addition of fetal bovine serum (FBS, 10%), L-glutamine (5 mM), streptomycin (100 μg $mL^{-1}$), and penicillin (100 U $mL^{-1}$) (Sigma–Aldrich), and incubated at 37 °C in a 5% $CO_2$ controlled atmosphere. For the cytotoxicity assay, the medium was removed from the flask, and the cells washed with 6 mL of PBS, and then shaken in the presence of 1 mL of trypsin (Sigma–Aldrich), with 3 min incubation. LG-DMEM was successively added, and the obtained cellular suspension seeded in 96-well microplates ($8\times10^3$ cells per well) in the growth medium (200 μL) and incubated at 37 °C in a 5% $CO_2$ atmosphere for 24 h to allow cell adhesion, prior to drug testing. The ionic $Au^{III}$ complexes of the type [1:2]Cl and the $Cu^{II}$ glycosylated derivatives, which are all water soluble, were dissolved in saline solution (NaCl 0.9% *w/v*). All compounds were tested against the HCT116 cells at various micromolar concentrations to obtain dose–response plots. Briefly, the metal derivatives were dissolved in saline at concentrations of 50, 25, 10, 5, 2, 1, and 0.5 mM. Successively, each solution (1 μL) was dissolved in 999 μL of cell culture medium (LG-DMEM), to yield the following final concentrations of metal complex: 50, 25, 10, 5, 2, 1, and 0.5 μM. After preparation of the 96-well plates, containing 8000 cells each, the medium was removed and replaced with fresh medium containing the compounds to be studied at increasing concentrations. Triplicate conditions were established for each treatment, and six independent experiments were carried out for each compound. Mitochondrial cell viability was evaluated by means of resazurin assay. To perform the assay, the entire volume of incubation medium was removed after 72 h from the treated wells, and 100 μL per well of a 10% resazurin solution in LG-DMEM were added and incubated for 2 h at 37 °C. The control cells were those treated with cell culture medium. The obtained cell viabilities were plotted against the compound concentration to determine the $IC_{50}$ value (concentration of the test agent inducing 50% decrease in cell number relative to control cell cultures). The final $IC_{50}$ values and their standard deviations were evaluated from the data coming from at least three independent experiments. For comparison purposes, the cytotoxicity of cisplatin (dissolved in saline solution) was evaluated under the same experimental conditions. In this regard, it should be noted that the experiments were performed over a period of 72 h, as this is the time necessary for cisplatin to effect its activity. To perform experiments with inhibitors, a procedure similar to those reported by Gao and Lippard were followed. *O*-Ethylidene-α-D-glucose was dissolved in 999 μL of cell culture medium at a concentration 10 mM prior to addition of the complex.[22] Conversely, phlorizin dihydrate, due to its low solubility, was previously dissolved in DMSO at a concentration of 1 M. Successively, 1 μL of the solution was dissolved in 999 μL of cell culture medium (LG-DMEM), to yield the following final concentrations of 1 mM of the inhibitors in each well.[16] This procedure results in a DMSO concentration of 0.01% *v/v* in the growth medium, which has no effect on cell viability.[81] The competitor D-glucose was dissolved in culture medium at a concentration of 50 mM prior to drug addition.

## Acknowledgements

*This work was supported financially by T.R.N.–Imballaggi Logistics Services (PhD fellowship to N.P., www.trnimballaggi.it/en/), the University of Padua (postdoctoral fellowship to C.N., "Assegno di Ricerca Senior" area scientifica di ateneo no. 03—Scienze chimiche), and the L'Oréal Foundation–UNESCO (postdoctoral fellowship to C.N., www.forwomeninscience.com/en/fellowships).*

## Conflict of interest

*The authors declare no conflict of interest.*

**Keywords:** carbohydrates · copper · gold · dithiocarbamates · metal complexes

[1] "Key Facts on Cancer", World Health Organization (WHO), http://www.who.int/news-room/fact-sheets/detail/cancer, September 12, 2018.
[2] "Cancer Tomorrow: A tool that predicts the future cancer incidence and mortality burden worldwide from the current estimates in 2018 up until 2040", International Agency for Research on Cancer (IARC), http://gco.iarc.fr/tomorrow/home, 2018.
[3] a) S. Monro, K. L. Colón, H. Yin, J. Roque III, P. Konda, S. Gujar, R. P. Thummel, L. Lilge, C. G. Cameron, S. A. McFarland, *Chem. Rev.* **2019**, *119*, 797–828; b) X. Wang, X. Wang, S. Jin, N. Muhammad, Z. Guo, *Chem. Rev.* **2019**, *119*, 1138–1192.
[4] E. C. Calvaresi, P. J. Hergenrother, *Chem. Sci.* **2013**, *4*, 2319–2333.
[5] I. R. Vlahov, C. P. Leamon, *Bioconjugate Chem.* **2012**, *23*, 1357–1369.
[6] E. I. Vrettos, G. Mező, A. G. Tzakos, *Beilstein J. Org. Chem.* **2018**, *14*, 930–954.

[7] W. X. Ren, J. Han, S. Uhm, Y. J. Jang, C. Kang, J.-H. Kim, J. S. Kim, *Chem. Commun.* **2015**, *51*, 10403 – 10418.
[8] S. Xing-Dong, K. Xia, H. Shu-Fen, C. Jia-Xi, S. Jing, C. Bing-Bing, Z. Jin-Wu, M. Zong-Wan, *Eur. J. Med. Chem.* **2017**, *138*, 246 – 254.
[9] O. Warburg, K. Posener, E. Negelein, *Biochem. Z.* **1924**, *152*, 319 – 344.
[10] O. Warburg, *Science* **1956**, *123*, 309 – 314.
[11] J. Zheng, *Oncol. Lett.* **2012**, *4*, 1151 – 1157.
[12] R. J. DeBerardinis, N. S. Chandel, *Sci. Adv.* **2016**, *2*, e1600200.
[13] R. A. Medina, G. I. Owen, *Biol. Res.* **2002**, *35*, 9 – 26.
[14] Z. Tan, C. Yang, X. Zhang, P. Zheng, W. Shen, *Oncotarget* **2017**, *8*, 60954 – 60961.
[15] J. Yang, J. Wen, T. Tian, Z. Lu, Y. Wang, Z. Wang, X. Wang, Y. Yang, *Oncotarget* **2017**, *8*, 11788 – 11796.
[16] P. Liu, Y. Lu, X. Gao, R. Liu, D. Zhang-Negrerie, Y. Shi, Y. Wang, S. Wanga, Q. Gao, *Chem. Commun.* **2013**, *49*, 2421 – 2423.
[17] H. Li, X. Gao, R. Liu, W. Yu, M. Zhang, Z. Fu, Y. Mi, Y. Wang, Z. Yao, Q. Gao, *Eur. J. Med. Chem.* **2015**, *101*, 400 – 408.
[18] Q. Mi, Y. Ma, X. Gao, R. Liu, P. Liu, Y. Mi, X. Fu, Q. Gao, *J. Biomol. Struct. Dyn.* **2016**, *34*, 2339 – 2350.
[19] M. Wu, H. Li, R. Liu, X. Gao, M. Zhang, P. Liu, Z. Fu, J. Yang, D. Zhang-Negrerie, Q. Gao, *Eur. J. Med. Chem.* **2016**, *110*, 32 – 42.
[20] X. Gao, S. Liu, Y. Shi, Z. Huang, Y. Mi, Q. Mi, J. Yang, Q. Gao, *Eur. J. Med. Chem.* **2017**, *125*, 372 – 384.
[21] M. Patra, S. G. Awuah, S. J. Lippard, *J. Am. Chem. Soc.* **2016**, *138*, 12541 – 12551.
[22] M. Patra, T. C. Johnstone, K. Suntharalingam, S. J. Lippard, *Angew. Chem. Int. Ed.* **2016**, *55*, 2550 – 2554; *Angew. Chem.* **2016**, *128*, 2596 – 2600.
[23] C. Nardon, D. Fregona, *Curr. Top. Med. Chem.* **2016**, *23*, 360 – 380.
[24] L. Brustolin, C. Nardon, N. Pettenuzzo, N. Zuin Fantoni, S. Quarta, F. Chiara, A. Gambalunga, A. Trevisan, L. Marchiò, P. Pontisso, D. Fregona, *Dalton Trans.* **2018**, *47*, 15477 – 15486.
[25] M. Altaf, A. A. Isab, J. Vančo, Z. Dvořák, Z. Trávníček, H. Stoeckli-Evans, *RSC Adv.* **2015**, *5*, 81599 – 81607.
[26] J. C. García-Ramos, A. G. Gutièrrez, A. Vàzquez-Aguirre, Y. Toledano-Magaña, A. L. Alonso-Sàenz, V. Gomez-Vidales, M. Flores-Alamo, C. Mejìa, L. Ruiz-Azuara, *BioMetals* **2017**, *30*, 43 – 58.
[27] B. Bertrand, A. Citta, I. L. Franken, M. Picquet, A. Folda, V. Scalcon, M. P. Rigobello, P. Le Gendre, A. Casini, E. Bodio, *J. Biol. Inorg. Chem.* **2015**, *20*, 1005 – 1020.
[28] M. N. Wenzel, A. F. Mósca, V. Graziani, B. Aikman, S. R. Thomas, A. De Almeida, J. A. Platts, N. Re, C. Coletti, A. Marrone, G. Soveral, A. Casini, *Inorg. Chem.* **2019**, *58*, 2140 – 2148.
[29] G. Boscutti, C. Nardon, L. Marchiò, M. Crisma, B. Biondi, D. Dalzoppo, L. Dalla Via, F. Formaggio, A. Casini, D. Fregona, *ChemMedChem* **2018**, *13*, 1131 – 1145.
[30] M. F. Tomasello, C. Nardon, V. Lanza, G. Di Natale, N. Pettenuzzo, S. Salmaso, D. Milardi, P. Caliceti, G. Pappalardo, D. Fregona, *Eur. J. Med. Chem.* **2017**, *138*, 115 – 127.
[31] C. Nardon, N. Pettenuzzo, D. Fregona, *Curr. Med. Chem.* **2016**, *23*, 3374 – 3403.
[32] Z. Molphy, D. Montagner, S. S. Bhat, C. Slator, C. Long, A. Erxleben, A. Kellett, *Nucleic Acid Res.* **2018**, *46*, 9918 – 9931.
[33] G. Hogarth, *Mini Rev. Med. Chem.* **2012**, *12*, 1202 – 1215.
[34] D. Deng, P. Sun, C. Yan, M. Ke, X. Jiang, L. Xiong, W. Ren, K. Hirata, M. Yamamoto, S. Fan, N. Yan, *Nature* **2015**, *526*, 391 – 396.
[35] D. Deng, N. Yan, *Protein Sci.* **2016**, *25*, 546 – 558.
[36] A. M. Navale, A. N. Paranjape, *Biophys. Rev. Lett.* **2016**, *8*, 5 – 9.
[37] M. Mueckler, B. Thorens, *Mol. Aspects Med.* **2013**, *34*, 121 – 138.
[38] E. Fischer, *Ber. Dtsch. Chem. Ges.* **1893**, *26*, 2400 – 2412.
[39] W. Koenigs, E. Knorr, *Ber. Dtsch. Chem. Ges.* **1901**, *34*, 957 – 981.
[40] B. Helferich, K. F. Wedemeyer, *Liebigs Ann.* **1949**, *563*, 139 – 145.
[41] R. Šardzík, G. T. Noble, M. J. Weissenborn, A. Martin, S. J. Webb, S. L. Flitsch, *Beilstein J. Org. Chem.* **2010**, *6*, 699 – 703.
[42] G. Magnusson, G. Noori, J. Dahmen, T. Frejd, T. Lave, *Acta Chem. Scand. B.* **1981**, *35*, 213 – 216.
[43] P. O. Adero, T. Furukawa, M. Huang, D. Mukherjee, P. Retailleau, L. Bohé, D. Crich, *J. Am. Chem. Soc.* **2015**, *137*, 10336 – 10345.
[44] L. Bohé, D. Crich, *Nat. Chem.* **2016**, *8*, 99 – 100.
[45] B. Ren, M. Wang, J. Liu, J. Ge, X. Zhang, H. Dong, *Green Chem.* **2015**, *17*, 1390 – 1394.
[46] L. Ronconi, C. Maccato, D. Barreca, R. Saini, M. Zancato, D. Fregona, *Polyhedron* **2005**, *24*, 521 – 531.
[47] A. Nickon, M. A. Castle, R. Harada, C. E. Berkoff, R. O. Williams, *J. Am. Chem. Soc.* **1963**, *85*, 2185 – 2186.
[48] J. B. Lambert, J. E. Goldstein, *J. Am. Chem. Soc.* **1977**, *99*, 5689 – 5693.
[49] D. A. Brown, W. K. Glass, M. A. Burke, *Spectrochim. Acta Part A* **1976**, *32*, 145 – 147.
[50] K. J. Cavell, J. O. Hill, R. J. Magee, *J. Inorg. Nucl. Chem.* **1979**, *41*, 1277 – 1280.
[51] L. Giovagnini, S. Sitran, M. Montopoli, L. Caparrotta, M. Corsini, C. Rosani, P. Zanello, Q. P. Dou, D. Fregona, *Inorg. Chem.* **2008**, *47*, 6336 – 6343.
[52] F. Forghieri, C. Preti, L. Tassi, G. Tosi, *Polyhedron* **1988**, *7*, 1231 – 1237.
[53] R. Varma, S. Y. Kulkarni, C. I. Jose, V. S. Pansare, *Carbohydr. Res.* **1984**, *133*, 25 – 32.
[54] R. S. Tipson, *Infrared Spectroscopy of Carbohydrates: a Review of the Literature*, National Bureau of Standards Monographs, **1966**, p. 13 – 14.
[55] S. Synytsya, M. Novak, *Ann. Transl. Med.* **2014**, *2*, 17 – 31.
[56] P. T. Beurskens, J. A. Cras, J. G. M. Van der Linden, *Inorg. Chem.* **1970**, *9*, 475 – 479.
[57] A. R. Hendrickson, R. L. Martin, N. M. Rohde, *J. Am. Chem. Soc.* **1976**, *98*, 2115 – 2119.
[58] A. R. Hendrickson, R. L. Martin, D. Taylor, *J. Chem. Soc. Chem. Commun.* **1975**, 843 – 844.
[59] R. Turnaturi, V. Oliveri, M. Viale, M. Monticone, G. Vecchio, *ChemPlusChem* **2015**, *80*, 1786 – 1792.
[60] N. N. Murthy, K. D. Karlin, I. Bertini, C. Luchinat, *J. Am. Chem. Soc.* **1997**, *119*, 2156 – 2162.
[61] K. Nakamoto, J. Fujita, R. A. Condrate, Y. Morimoto, *J. Chem. Phys.* **1963**, *39*, 423 – 427.
[62] C. N. R. Rao, R. Venkataraghavan, *Spectrochim. Acta* **1962**, *18*, 541 – 547.
[63] R. Kellner, G. S. Nikolov, N. Trendafilova, *Inorg. Chim. Acta* **1984**, *84*, 233 – 239.
[64] F. Bonati, R. Ugo, *Organomet. Chem.* **1967**, *10*, 257 – 268.
[65] R. Kellner, G. S. Nikolov, *J. Inorg. Nucl. Chem.* **1981**, *43*, 1183 – 1188.
[66] P. D. Leeson, B. Springthorpe, *Nat. Rev. Drug Discovery* **2007**, *6*, 881 – 890.
[67] F. Esteves, C. Moutinho, C. Matos, *J. Liposome Res.* **2013**, *23*, 83 – 93.
[68] T. Marzo, S. Pillozzi, O. Hrabina, J. Kasparkova, V. Brabec, A. Arcangeli, G. Bartoli, M. Severi, A. Lunghi, F. Totti, C. Gabbiani, A. G. Quiroga, L. Messori, *Dalton Trans.* **2015**, *44*, 14896 – 14905.
[69] M. F. Mazzobre, M. V. Romàn, A. F. Mourelle, H. R. Corti, *Carbohydr. Res.* **2005**, *340*, 1207 – 1211.
[70] P. T. Beurskens, H. J. A. Blaauw, J. A. Cras, J. J. Steggerda, *Inorg. Chem.* **1968**, *7*, 805 – 810.
[71] C. K. Jørgensen, *J. Inorg. Nucl. Chem.* **1952**, *24*, 1571 – 1585.
[72] F. Takami, S. Wakahara, T. Maeda, *Tetrahedron Lett.* **1971**, *12*, 2645 – 2648.
[73] S. Choi, E. R. Menzel, J. R. Wasson, *J. Inorg. Nucl. Chem.* **1977**, *39*, 417 – 422.
[74] D. J. Berry, R. T. M. de Rosales, P. Charoenphun, P. J. Blower, *Mini Rev. Med. Chem.* **2012**, *12*, 1174 – 1183.
[75] P. Lopez-Serra, M. Marcilla, A. Villanueva, A. Ramos-Fernandez, A. Palau, L. Leal, J. E. Wahi, F. Setien-Baranda, K. Szczesna, C. Moutinho, A. Martinez-Cardus, H. Heyn, J. Sandoval, S. Puertas, A. Vidal, X. Sanjuan, E. Martinez-Balibrea, F. Vinals, J. C. Perales, J. B. Bramsem, T. F. Ørntoft, C. L. Andersen, J. Tabernero, U. McDermott, M. B. Boxer, M. G. Vander Heiden, J. Pablo Albar, M. Esteller, *Nat. Commun.* **2014**, *5*, 3608.
[76] S. C. Rumsey, O. Kwon, G. W. Xu, C. F. Burant, I. Simpson, M. Levine, *J. Biol. Chem.* **1997**, *272*, 18982 – 18989.
[77] A. Malhotra, S. Kudyar, A. K. Gupta, R. P. Kudyar, P. Malhotra, *Int. J. Appl. Basic Med. Res.* **2015**, *5*, 161 – 163.
[78] N. Michihata, Y. Kaneko, Y. Kasai, K. Tanigawa, T. Hirokane, S. Higasa, H. Yamada, *J. Org. Chem.* **2013**, *78*, 4319 – 4328.
[79] N. C. Baenziger, W. E. Bennett, D. M. Soboroff, P. F. O'Donnell, J. R. Doyle, *Polyhedron* **1998**, *17*, 2379 – 2410.
[80] A. Leyva, X. Zhang, A. Corma, *Chem. Commun.* **2009**, 4947 – 4949.
[81] G. Da Violante, N. Zerrouk, I. Richard, G. Provot, J. C. Chaumeil, P. Arnaud, *Biol. Pharm. Bull.* **2002**, *25*, 1600 – 1603.

Manuscript received: April 11, 2019
Revised manuscript received: April 29, 2019
Accepted manuscript online: ■■ ■■, 0000
Version of record online: ■■ ■■, 0000

*N. Pettenuzzo, L. Brustolin, E. Coltri, A. Gambalunga, F. Chiara, A. Trevisan, B. Biondi, C. Nardon, D. Fregona**

■■ – ■■

**$Cu^{II}$ and $Au^{III}$ Complexes with Glycoconjugated Dithiocarbamato Ligands for Potential Applications in Targeted Chemotherapy**


**Energy-hungry cells, beware:** This work is focused on the synthesis, characterization, and preliminary anticancer activity evaluation of carbohydrate-conjugated $Au^{III}$ and $Cu^{II}$ dithiocarbamato complexes, with the aim of improving the selective accumulation of the metal payload into malignant cells by exploiting the well-known Warburg effect.